

GLIN: A Lightweight Learned Indexing Mechanism for Complex Geometries

Congying Wang
Washington State University
congying.wang@wsu.edu

Jia Yu
Washington State University
jia.yu1@wsu.edu

Abstract—Although spatial index structures shorten the query response time, they rely on complex tree structures to narrow down the search space. Such structures in turn yield additional storage overhead and take a toll on index maintenance. Recently, there has been a flurry of works attempting to leverage Machine-Learning (ML) models to simplify the index structures. Some follow-up works extend the idea to support geospatial point data. These approaches partition the multidimensional space to cells and assign IDs to these cells using space-filling curve (e.g., Z-order curve) or mathematical equations. These approaches work well for geospatial points but are not able to handle complex geometries such as polygons and trajectories which are widely available in geospatial data.

This paper introduces GLIN, a lightweight learned index for spatial range queries on complex geometries. To achieve that, GLIN transforms geometries to Z-address intervals, and builds a hierarchical model to learn the cumulative distribution function between these intervals and the record positions. The lightweight hierarchical model greatly shortens the index probing time. Furthermore, GLIN augments spatial query windows using an add-on function to guarantee the query accuracy for both *Contains* and *Intersects* spatial relationships. Our experiments on real-world and synthetic datasets show that GLIN occupies 40 - 70 times less storage overhead than popular spatial indexes such as Quad-Tree while still showing similar query response time in medium selectivity queries. Moreover, GLIN's maintenance speed is around 1.5 times higher on insertion and 3 - 5 times higher on deletion.

I. INTRODUCTION

Database Management Systems (DBMSs) often create spatial indexes such as R-Tree [1], KD-Tree [2], and Quad-Tree [3] to accelerate queries on geospatial data. Although spatial index structures shorten query response time, they rely on complex tree structures to narrow down the search space. Such structures in turn yield additional storage overhead and take a toll on index maintenance [4]. Recent works on spatial indices [5], [6] mostly focus on accelerating query speed at the cost of even higher storage overhead. As depicted in Table Ia, R-Tree and Quad-Tree usually cost 10% - 20% additional storage overhead. This leads to significant dollar cost especially now that most enterprises move their data to cloud storage for better security and stability. Table Ib shows the cloud storage cost we collect from Amazon Web Services (AWS) EC2, the most popular cloud vendor. Such storage services are typically charged on a monthly or even an hourly basis, with additional fees for data transfer, which can result in unexpected bills for the users.

TABLE I: Index storage overhead and storage dollar cost

(a) Index storage overhead on geospatial data (described in Table IV)

	Boost R-Tree	GEOS Quad-Tree
ROADS (8.3GB)	1.57GB	1.98GB
LinearWater (6.4GB)	461.1 MB	685 MB
Parks (8.5GB)	783 MB	1.01GB

(b) Cloud storage cost on Amazon Web Services EC2 instances

RAM (no. CPU)	SSD storage	Data transfer
32GB (2): \$0.16/hour	L1: \$0.08/GB/month	Internal 1: \$0.01/GB
64GB (4): \$0.33/hour	L2: \$0.10/GB/month	Internal 2: \$0.02/GB
128GB (8): \$0.66/hour	L3: \$0.12/GB/month	External: \$0.09/GB

With the wide adoption of open-source and shareable data formats including Apache Parquet [7], GeoParquet [8], Delta Lake [9] and Apache Iceberg [10], and the emergence of modern hardware such as SSD and Non-Volatile Memory, many DBMSs shift their attentions to utilizing the increasing hardware bandwidth to bolster fast data scanning with the assistance of lightweight index structures. Several works in this field have proposed to leverage data synopses such as min-max, bounding box, and histograms [4], [11]–[13] from the indexed data to navigate queries to desired locations. They adopt a much simpler data structure, which brings down the cost of storing and maintaining the index. However, they compromise on query response time and cannot be easily tailored to geospatial data (e.g., polygons, trajectories, ...).

Recently, there has been a flurry of works [14]–[16] attempting to leverage Machine-Learning (ML) models to simplify the index structures. An index, denoted as $y = f(x)$, is a ML model inherently, where x is the lookup key and y is the physical position of the complete record. Theoretically, this ML model learns the Cumulative Distribution Function (CDF) between keys and their positions in a sorted array. Although learned index structures demonstrate promising results on space saving and query speedup as opposed to the traditional B+ Tree index, these approaches only work for 1 dimensional sortable point data.

To remedy that, some follow-up works extend the idea to support geospatial points. These approaches [17]–[20] partition the multidimensional space to cells and assign IDs to these cells using space-filling curve (e.g., Z-order curve [19]) or mathematical equations [18]. This way, they can reduce data dimension and hence enable the ML model training. These approaches work well for geospatial points but are incapable of

handling complex geometries such as polygons and trajectories which are widely available in geospatial data. One reason is that complex geometries can intersect multiple cells and thus have more than one ID. This leads to duplicates in the final result [21] and hence GLIN returns inaccurate results. In addition, the user must hand-tune the partitioning resolution to find an appropriate cell size that is small enough but also does not introduce too many duplicates. Finding such a sweet spot can be prohibitively expensive especially when indexed geometries go across large regions by nature (e.g., trajectories).

Designing a learned index structure for complex geometries presents several major challenges, stated as follows: (1) *Shapes*. Geometries are collections of various complex shapes including polygons and trajectories, which have been standardized to 7 categories [22]. No CDF is directly available between geometries and their positions. (2) *Spatial distribution*. Geometries often show specific spatial distributions in the space. For example, most landmarks, such as parks, hospitals, and government buildings, cluster at major metropolitan regions. The index structures should adapt to such distributions for better prediction performance. (3) *Spatial relationship*. Geometries may have various spatial relationships such as *Contains*, *Intersects*, *Touches*, and *Disjoint*. Given a spatial query, the learned index structures must identify the specified spatial relationship and guarantee the query accuracy.

This paper proposes GLIN¹, a lightweight learned indexing mechanism for spatial range queries on complex geometries such as points, polygons, and trajectories. GLIN by design produces low storage and maintenance overhead while achieving competitive query performance in common cases, as opposed to Quad-Tree and R-Tree. Moreover, GLIN can work in conjunction with existing regular learned indexes to enable geospatial data support. Our contributions in this paper are summarized as follows:

- GLIN transforms geometries to 1-dimensional sortable values, namely Z-address intervals, using Z-order curve. We prove that with query augmentation, GLIN can always deliver correct results for different spatial relationships.
- GLIN extends existing regular learned indexes to train hierarchical models on Z-address intervals and further improves the search performance by introducing additional information in leaf models. To the best of our knowledge, it is the first learned index that handles non-point values.
- GLIN equips efficient algorithms to update its index structure for data insertion and deletion while guaranteeing the query accuracy.
- Our experimental analysis on real-world and synthetic datasets shows that GLIN occupies 40 - 70 times less storage overhead than popular spatial indexes such as Quad-Tree while still showing competitive query response time on medium selectivity (0.1% - 1% selectivity), which indicates a metro area for USA-level data and is commonly used in spatial analytics applications. Moreover, as opposed to R-Tree and

Quad-Tree, GLIN's maintenance speed is around 1.5 times higher on insertion and 3-5 times higher on deletion.

The remainder of this paper is structured as follows: In Section II, we present the necessary background knowledge for geospatial queries. The key ideas of GLIN are listed in Section III. In Section IV - VII, we explain how to initialize the index, search the index, and maintain it efficiently. Section VIII introduces the query augmentation of GLIN for handling *Intersects* spatial relationship. Extensive experimental evaluation is presented in Section IX. We summarize the related work in Section X. Finally, Section XI concludes the paper.

II. BACKGROUND

Spatial range query. Given a query window Q , a spatial dataset R and a predefined spatial relationship SR , a range query denoted as $range(Q, R, SR)$ finds the geometries in R such that each geometry (denoted as GM) has SR relationship with Q . GM and Q can have any shapes including polygons and lines.

Spatial relationship. SQL/MM3 standard [22] lists a number of possible spatial relationships between two geometries. This includes but is not limited to: *Contains*, *Intersects*, *Touches*, and *Disjoint*. In this paper, we focus on two most common spatial relationships: (1) *Contains* (Figure 2 Case 1): given two geometries Q and GM , "Q contains GM" is true if and only if no points of GM lie in the exterior of Q , and at least one point of the interior of GM lies in the interior of Q . (2) *Intersects* (Figure 2 Case 1, 2, 3): given two geometries Q and GM , "Q intersects GM" is true if Q and GM share any portion of space. *Contains* is a special case of *Intersects*. If "Q contains GM" is true, then "Q intersects GM" must be true as well.

Minimum Bounding Rectangle (MBR). A MBR describes the maximum extents of a 2-dimensional geometry in a (x, y) coordinate system. A MBR consists of four values, the minimum and maximum values of x and y coordinates of a geometry, and are represented as two points, $p_{min}(x_{min}, y_{min})$ and $p_{max}(x_{max}, y_{max})$ (see Figure 2 Case 1). The coordinates of MBR can be easily obtained by iterating every coordinate of this geometry. MBR is often used to approximate geometries since it is a much simpler shape.

Probing and Refinement steps of spatial index search. Most existing spatial indexing mechanisms, such as R-Tree, Quad-Tree, and KD-Tree, approximate complex geometries to their MBR and then build index structures on MBRs. A spatial range query is processed mostly in two steps. (1) *Indexprobing*: the MBR of the query window is processed against the spatial index. It returns a set of candidate geometries whose MBRs possibly *intersect* the query window MBR. This set of candidates is not the exact answer of this query but is a super set of the answer. (2) *Refinement*: the candidate geometries are checked against the query window using their actual shapes with a spatial relationship such as *Contains* or *Intersects*. The refinement step is computationally expensive due to the complexity of shapes and usually takes more time than the filter step [23]. GLIN also

¹GLIN GitHub repository: <https://github.com/DataOceanLab/GLIN>

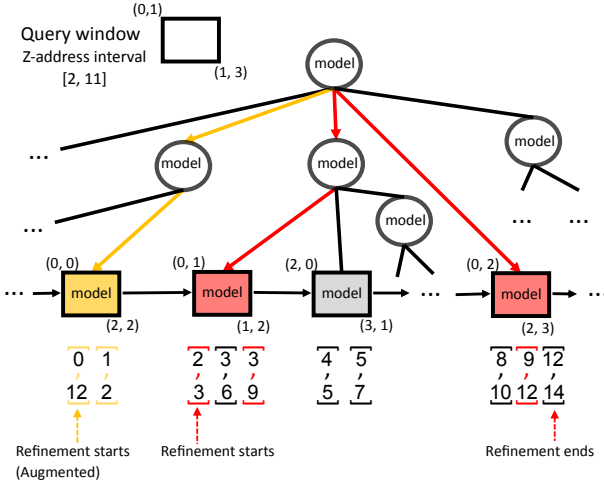


Fig. 1: GLIN index structure. White nodes are internal nodes and colored nodes are leaves. Index search: (1) *Contains*: follow the red paths and return red records. The gray node is skipped as its MBR does not intersect the query. (2) *Intersects*: follow the yellow path and the second red path. Red and yellow records will be returned.

follows this two-step process which can significantly reduce computation cost and index storage overhead.

III. OVERVIEW

The index structure of GLIN is depicted in Figure 1.

Z-address interval. Existing learned indexing mechanisms are theoretically based on the presence of a CDF between keys and record positions. Geometries, on the other hand, can feature multidimensional shapes, such as polygons and lines, which cannot be arranged in a sequential order. Therefore we cannot see such CDF on geometry keys. To establish this CDF and enable the model training process, GLIN assigns each geometry a Z-address interval, an one-dimensional sortable interval (serve as keys), by using a well-known space-filling curve called Z-order curve. In this paper, we also study that how *Contains* and *Intersects* relationships are reflected on Z-address intervals and prove that GLIN can guarantee the query accuracy in both cases.

Index structure. Once the CDF is made available between Z-address intervals and record positions, GLIN can harness the model training approach of existing learned indexes such as RMI [14], ALEX [16], and RadixSpline [24]. In this paper, it extends ALEX to build a hierarchical model to learn the CDF. Since Z-address intervals cannot 100% preserve the original shape information and spatial proximity, the index probing will return some false positive results. In response, GLIN introduces a refinement phase to prune out all false positives. In addition, it creates a MBR on each leaf node of the hierarchical model to accelerate the refinement phase.

Query augmentation. The basic indexing mechanism in GLIN is designed to handle *Contains* relationship and may produce true negatives for *Intersects* relationship. To remedy

TABLE II: Notations used in this paper

Term	Definition
Q, GM	Q - a spatial range query window. GM - an indexed geometry. Both can be in any shapes.
MBR	Minimum Bounding Rectangle of a geometry, represented as two points $p_{min}(x_{min}, y_{min})$ and $p_{max}(x_{max}, y_{max})$ MBR_Q - MBR of Q. MBR_{GM} - MBR of GM.
Zmin	Z-address for p_{min} of a MBR $Zmin_Q$ - Zmin of Q, $Zmin_{GM}$ - Zmin of GM.
Zmax	Z-address for p_{max} of a MBR $Zmax_Q$ - Zmax of Q, $Zmax_{GM}$ - Zmax of GM.
Zitvl	Z-address interval described by $[Zmin, Zmax]$ $Zitvl_Q$ - Zitvl of Q, $Zitvl_{GM}$ - Zitvl of GM.

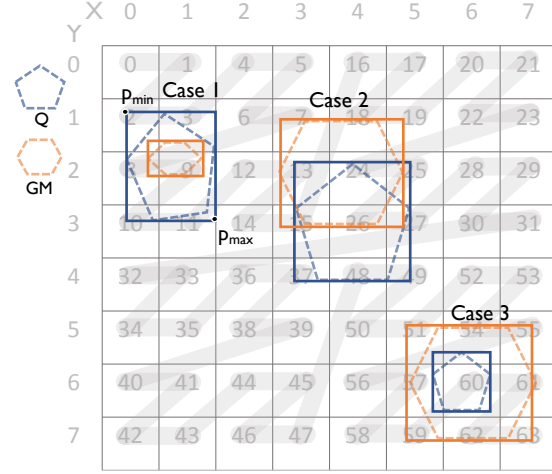


Fig. 2: Spatial relationship. Case 1: Q *contains* GM; Case 1, 2, 3: Q *intersects* GM. Z-address(p_{min}) = 2, Z-address(p_{max}) = 11, Z-address interval of Q in Case 1 = [2, 11].

that, GLIN employs a simple piecewise function as an add-on component to augment the query window. More precisely, GLIN will enlarge the Z-address interval of the query window to make sure that it covers all correct results at the cost of additional pruning time.

IV. Z-ADDRESS INTERVALS OF GEOMETRIES

This section describes how GLIN assigns Z-address interval to geometries (see Figure 2). Notations used in this section are summarized in Table II.

Z-address. We can imagine a Z-order curve as a Z-shape curve that connects all 2-dimensional positive integer coordinates in the space. Each coordinate (x, y) will then have a Z-address and such values of two nearby coordinates will likely be close to each other. For example, $p_{min}(0, 1)$ in Figure 2 will have a Z-address 2. GLIN rounds down geospatial coordinates to their nearest integers: $x = \frac{\text{longitude} - (-180^\circ)}{\text{cell size}}$ and $y = \frac{\text{latitude} - (-90^\circ)}{\text{cell size}}$. Then it calculates the Z-address using libmorton [25] which interleaves the binary representation of x and y coordinates [26]. Cell size can be any small number with 7 to 8 decimal places (see Figure 3). This way, we can minimize the situations that multiple geospatial coordinates have the same Z-address, which otherwise will affect the CDF. GLIN selects $5 * 10^{-7}$ to indicate centimeter-level precision [27].

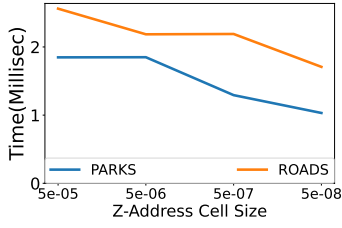


Fig. 3: Query time per cell size

Z-address interval. GLIN assigns a Z-address interval, $Zitvl[Zmin, Zmax]$, for every geometry including the indexed geometries and the range query window. This interval is calculated in two steps (1) Find the MBR of a geometry, represented by $p_{min}(x_{min}, y_{min})$ and $p_{max}(x_{max}, y_{max})$. (2) Get the minimum Z-address, $Zmin$ by assigning Z-address to p_{min} , and get the maximum Z-address, $Zmax$, by assigning Z-address to p_{max} . In Figure 2 Case 1, Q has $Zitvl_Q[2, 11]$.

Notes. (1) When calculating $Zitvl$, GLIN must use p_{min} and p_{max} rather than vertices of the geometry because $Zitvl$ from the latter might not cover all Z-addresses touched by the geometry. For example, vertices of Q in Figure 2 Case 1 indicate $Zitvl = [3, 11]$, which misses Z-address 2. (2) We choose Z-order curve due to its monotonic ordering property [26] which guarantees that $Zitvl$ from p_{min} and p_{max} covers the Z-address of any point that falls inside this geometry [19]. In Hilbert curve (or other space filling curves), the $Hmin$ and $Hmax$ of the desired $Hitvl$ are actually on the boundary of the MBR (details omitted due to page limit). To obtain such $Hitvl$, we have to calculate every H-address touched by the MBR. This will significantly slow down the queries and require to tune the cell size which cannot be too large or too small.

Theorem 1. Monotonic ordering [26]: Data points ordered by non-descending Z-addresses are monotonic in a way that a dominating point is placed before its dominated points.

where dominance is defined as: given two points p and p' , if p is no larger than p' in any dimension, then we say p dominates p' .

Spatial relationship between intervals. Because GLIN is built on Z-address intervals, when we examine the spatial relationship between Q and GM, we also need to understand how this relationship is reflected on the relationship between Z-address intervals of Q and GM, denoted as $Zitvl_Q$ and $Zitvl_{GM}$, respectively.

Lemma 1. Z-address interval Contains. If Q contains GM, then $Zitvl_Q$ contains $Zitvl_{GM}$

where " $Zitvl_Q$ contains $Zitvl_{GM}$ " includes the following AND conditions: (1) $Zmin_Q \leq Zmin_{GM} \leq Zmax_Q$, AND, (2) $Zmin_Q \leq Zmax_{GM} \leq Zmax_Q$.

To prove Lemma 1, we must first prove Theorem 2 since Z-address intervals are calculated based on MBRs.

Theorem 2. If Q contains GM, then MBR_Q contains MBR_{GM}

where MBR_Q contains MBR_{GM} is defined as: Q's p_{min} dominates GM's p_{min} and GM's p_{max} dominates Q's p_{max} .

Proof. Since Q contains GM, in a 2D space, if there is a line, it is obvious that the geometrical projection of Q on this line must contain the geometrical projection of GM on this line. In other words, when Q contains GM, then if a person stands somewhere outside Q, he or she should never see GM because GM is completely inside Q assuming Q is a closed geometry. The projection of a geometry on X axis and Y axis are $[x_{min}, x_{max}]$ and $[y_{min}, y_{max}]$, respectively. We have (1) Q's $x_{min} \leq GM's x_{min}$ & Q's $y_{min} \leq GM's y_{min}$, so Q's p_{min} dominates GM's p_{min} (2) GM's $x_{max} \leq Q's x_{max}$ & GM's $y_{max} \leq Q's y_{max}$, so GM's p_{max} dominates Q's p_{max} . \square

With Theorem 1 and 2, we are ready to prove Lemma 1.

Proof. $Zmin_{GM} \leq Zmax_{GM}$ is known. Since Q contains GM, we have (1) p_{min} of Q dominates p_{min} of GM, so $Zmin_Q \leq Zmin_{GM}$ (2) p_{max} of GM dominates p_{max} of Q, so $Zmax_{GM} \leq Zmax_Q$. \square

Lemma 2. Z-address interval Intersects. If Q Intersects GM, then $Zitvl_Q$ intersects $Zitvl_{GM}$

where " $Zitvl_Q$ intersects $Zitvl_{GM}$ " is defined as: $Zitvl_Q$ and $Zitvl_{GM}$ share some portion of the intervals. More precisely, this includes the following OR conditions: (1) $Zmin_Q \leq Zmin_{GM} \leq Zmax_Q$, OR, (2) $Zmin_Q \leq Zmax_{GM} \leq Zmax_Q$, OR, (3) $Zmin_{GM} \leq Zmin_Q$ AND $Zmax_Q \leq Zmax_{GM}$.

Proof. Since Q Intersects GM, Q and GM must share some portion of the space. On the other hand, Q and GM's $Zitvl$ guarantee to cover any point that falls inside Q and GM, respectively. Therefore, $Zitvl_Q$ and $Zitvl_{GM}$ share some portion of the intervals. \square

pdfoutput=1

V. INDEX INITIALIZATION

To create an index, GLIN reads a set of geometry records and initializes the index structure based on the geometries. The initialization phase consists of three steps: Step 1: sort geometries by their Z-address intervals; Step 2: build hierarchical models to learn the CDF between Z-address intervals and positions of records; Step 3: create a Minimum Bounding Rectangles (MBR) on each data node of GLIN. The mechanism depicted in this section only handles the spatial range query with the *Contains* spatial relationship, which is "the query window contains geometries".

A. Sort geometries by Z-address intervals

To establish the CDF between keys and record positions, the first step is to put the geometries in a sequential order. GLIN sorts geometries based on their Z-address intervals (see Section IV). The reason is two-fold: (1) Z-addresses can partially preserve the spatial proximity of geometries. This is critical because a spatial range query looks for geometries that

lie in the same region. This query will inevitably scan a large portion of the table if the trained ML model does not respect any spatial proximity. (2) A Z-address interval can partially preserve the shapes of geometries. This will make it possible for GLIN to employ different strategies for *Contains* and *Intersects* relationships for the sake of query performance.

GLIN iterates through every geometry and calculates the Z-address interval (i.e., $Z_{itvl} = [Z_{min}, Z_{max}]$) for this geometry. GLIN then sorts these geometries by the Z_{min} of their intervals. In the rest of the index initialization phase, Z_{max} of intervals will be completely discarded. In other words, GLIN actually indexes $\langle Z_{min}, \text{geometry key} \rangle$ pairs while traditional spatial indices index $\langle MBR, \text{geometry key} \rangle$ pairs. Later, in the index probing phase of the index search, GLIN only checks if the Z-address interval of the query window contains Z_{min} of geometries (i.e., $Z_{min_Q} \leq Z_{min_{GM}} \leq Z_{max_Q}$). According to Lemma 1, this introduces some false positive results but does not have true-negatives. Z_{max} will be used in Section VIII for query augmentation.

It is worth noting that GLIN could also sort geometries by the Z_{max} instead of Z_{min} . However, this will not make much difference in the learned CDF models since Z_{max} will follow the same data distribution of Z_{min} (see Figure 5). In Section VIII, both Z_{min} and Z_{max} will be needed in order to handle *Intersects* relationship.

B. Build a hierarchical model

Once geometries are sorted by the Z_{min} of their intervals, GLIN will train ML models to learn the CDF between these Z_{min} addresses and the record positions. GLIN can work in conjunction with an existing learned index and extend it to uphold geometries. Most existing learned indexes possess a hierarchical structure to build models for different regions. In this paper, we adopt the method in ALEX [16] because it supports index updates by design.

GLIN has a tree-like structure (see Figure 1) which consists of (1) internal nodes: each contains a linear regression model and an array of pointers to child nodes; and (2) leaf nodes: each contains a linear regression model, an array of actual data records and a MBR (elaborated in Section V-C). When given a key (Z_{min} value in our case), the model in each node will predict a position in the array, which leads to either the pointer of a child node, or a data record. Therefore the index probing in GLIN (see Section VI) is a tree traversal which starts from the root node and stops at a leaf node.

GLIN builds the hierarchical model in a top-down fashion, which is similar to a space-partitioning tree. It first splits the entire key space of all Z-addresses to many equal-width partitions and hence each partition may have different number of records. In each partition, GLIN trains a linear regression model to learn the CDF between Z-addresses and record positions in this partition. If the linear regression model is accurate enough, then these records and this model together compose a leaf node. Otherwise, GLIN further splits this partition to many multiple partitions and repeats the same process. The model in this partition and the pointers to those

child partitions compose an internal node. Each leaf node has a one-way pointer pointing to its next neighbor leaf node, which will be beneficial for the refinement step in the index search.

C. Create MBRs in leaf nodes

Since GLIN trains and queries models based on Z-addresses of geometries, the model prediction may introduce more false positives that need to be pruned during the refinement step.

To mitigate this, GLIN employs a simple yet efficient method to reduce the computation cost. When constructing each leaf node of the hierarchical model, GLIN also creates a MBR of all geometries in this node. This can be done by traversing all geometries and finding the overall $p_{min}(x_{min}, y_{min})$ and $p_{max}(x_{max}, y_{max})$. When refining the query results, GLIN will directly skip a leaf node unless the MBR of this node intersects the query window's MBR.

VI. INDEX SEARCH

Algorithm 1: GLIN Index Search

```

Input : A query window  $Q$ , a spatial relationship  $SR$ 
Output: A set of records  $Result$  that satisfy  $SR$  with  $Q$ 
1 /* Step 1: index probing */
2  $Z_{itvl_Q}[Z_{min}, Z_{max}] = \text{calculate\_zitvl}(Q)$ ;
3 if  $SR$  is "Intersects" relationship then
4   // Augment the query window
5    $Z_{min} = \text{augment}(Z_{itvl_Q}, \text{piecewise function}).Z_{min}$ ;
6  $\text{start\_position} = \text{model\_traversal}(\text{GLIN.root}, Z_{min})$ ;
7 /* Step 2: refinement */
8  $Result = \text{new List}()$ ;
9  $iterator = \text{start\_position}$ ;
10 while  $iterator.key \leq Z_{max}$  do
11    $geom = \text{Get\_Record}(iterator)$ ;
12   if  $Q$  has  $SR$  with  $geom$  then
13      $Result.add(geom)$ ;
14    $node = iterator.node()$ ;
15   if  $iterator \geq node.last\_position()$  then
16     while  $MBR_Q$  does not intersect  $node.MBR$  do
17        $node = node.next\_node()$ ; // Skip this node
18      $iterator = node.first\_position()$ ;
19   else
20      $iterator++$ ;
21 Return  $Result$ ;
22 Function  $\text{model\_traversal}(root, key)$ :
23    $node = root$ ;
24   while  $node.is\_leaf() == \text{false}$  do
25      $node = node.children[node.model.predict(key)]$ ;
26   Return  $node.expo\_search(node.model.predict(key))$ ;

```

The index search algorithm takes as input a spatial range query window and returns a set of records that satisfy the given spatial relationship with the query window. The algorithm runs through two main steps. (1) Index probing: probe GLIN's index structure to return a set of result candidates. (2) Refinement: filter the candidates to remove false positives. The search algorithm described in this section only handles the *Contains* spatial relationship.

A. Index probing

GLIN builds the hierarchical model based on the Z_{min} addresses of geometries. Therefore, to search the index, this algorithm must first obtain the Z-address interval of the query window (see Section IV). The Z-address interval $[Z_{min}, Z_{max}]$ of the query window will then serve as the actual input for the index probing which finds geometries whose Z_{min} is within the interval. According to Lemma 1, geometries whose Z_{min} is not within this interval are guaranteed not to be contained by the query window.

As described in Algorithm 1, the index probing step requires a tree-like traversal of the hierarchical model (i.e., *model_traversal*). It uses Z_{min} address of the query window as the lookup key (see the first red path in Figure 1). This traversal runs in a top-down fashion starting from the root. The model inside the root node will predict a position in the pointer array using the lookup key. The algorithm will then follow the pointer to a child node and repeat the same model prediction until it reaches a leaf node. The model prediction in each internal node has perfect accuracy thanks to the uniform partitioning in the index initialization algorithm, mitigating any need for additional search.

Once the algorithm reaches the leaf node, it will first perform the model prediction to find an approximate position in the record array and then run an exponential search from this position to locate the correct result. It is worth noting that the index probing is inherently a range search instead of an equality search. Therefore, when using the query window's Z_{min} as the input key, the traversal will return the pointer to the first record that is no less than this Z_{min} (similar to C++ `std::lower_bound`).

Complexity analysis. The cost of the *model_traversal* function is bounded by the depth of the hierarchical model. Assume m is the fanout of each internal node and p is the number of leaf nodes (each of which is a partition of the key space). Then *model_traversal* takes $O(\log_m p)$ in the worst case. The model-based exponential search in each leaf node costs $O(\log m)$ at worst.

B. Refinement

The records returned by the index probing have some false positives due to the following reasons: (1) GLIN uses the MBR of each geometry to produce the Z-addresses rather than the actual shape. (2) The Z address interval includes additional Z-addresses. For example, in Case 1 of Figure 2, the MBR_Q only contains 6 addresses (2, 3, 8, 9, 10, 11) but all records whose Z_{min} values are in [2, 11] (the Zitvl of Q, 10 Z-addresses in total) will be returned by the index probing step. (3) the hierarchical model is built upon the Z_{min} of geometries without considering Z_{max} at all.

As shown in Algorithm 1, GLIN conducts a refinement step to filter out these false positive results and hence guarantees the query accuracy. As illustrated in Figure 1, this refinement starts from the position returned by the Z_{min} -based model traversal and keeps checking if every geometry satisfies the spatial relationship with the query window using their exact

TABLE III: Number of records checked during the refinement

	Query selectivity	W/o leaf MBR	W/ leaf MBR
ROADS	1%	3339990	369184
	0.1%	1173710	67474
	0.01%	632839	18244
	0.001%	199923	6942
PARKS	1%	1126520	154685
	0.1%	291197	21700
	0.01%	105076	4180
	0.001%	45287	1451

shapes, until it arrives at the position whose key is no larger than the query window's Z_{max} .

During this process, every time when the algorithm arrives at the boundary of a leaf node, it will follow the pointer to the next leaf node. Before examining geometries in a leaf node, the algorithm first checks the MBR of this leaf node against the MBR of the query window. It will skip this leaf node if these two MBRs do not intersect, because geometries in this leaf node are guaranteed not to satisfy the spatial relationship with the window. For instance, the gray node in Figure 1 is skipped because its MBR $p_{min}(2, 0), p_{max}(3, 1)$ does not intersect the query window's MBR $p_{min}(0, 1), p_{max}(1, 3)$. As shown in Table III, this technique reduces the number of records checked in the refinement by up to 20 times compared to the one without leaf node MBRs.

VII. INDEX MAINTENANCE

GLIN will update its index structure when the underlying data receives insertion and deletion. For insertion, GLIN takes as input a geometry key and inserts it to the index. For deletion, the input is a geometry key and GLIN deletes records that have the same key.

Insertion. To insert a new record, GLIN first obtains the Z_{min} address for the geometry key in this record using the approach described in Section IV. It then traverses the hierarchical model to find a place in the leaf node record array. This process leverages the *model_traversal* in Algorithm 1 which runs in a top-down fashion starting from the root node. Once GLIN puts the new record in a leaf node, it expands the MBR of the leaf node to include the new geometry.

Deletion Similar to the insertion, the first step to delete a geometry key is to get the Z_{min} address of this geometry. GLIN then runs the same *model_traversal* in Algorithm 1 to perform the key lookup. It is possible that several different geometries share the same Z_{min} addresses. In that case, GLIN only erases records that have the same geometry key. The MBR of the involved leaf node will not be shrunk after the deletion because it requires a scan of all records in this leaf node to get the latest MBR. However, this does not affect the correctness of GLIN as the out-of-date MBR only introduces more false positives instead of true negatives.

Node expanding, splitting and merging. When a leaf node is close to be full (controlled by a upper density limit), GLIN will expand or split this leaf node as described in ALEX [16]. When a leaf node is close to be empty (controlled by a lower density limit), GLIN will merge this node with its sibling and the merged node will have a new MBR. The details of density

limits and the related cost model are beyond the scope of this paper and can be found in [16].

VIII. QUERY AUGMENTATION

The mechanism introduced in Section VI essentially finds geometries whose $Zmin$ address is in the Z-address interval of the query window. Thanks to Lemma 1, this correctly handles the *Contains* spatial relationship (e.g., Case 1 in Figure 2). However, it fails to uphold the *Intersects* spatial relationship since the less strict conditions in Lemma 2 bring in more qualified geometries. For example, the index search algorithm will miss Case 2 and 3 in Figure 2. The root cause is that the $Zmin$ addresses of qualified geometries lie outside the original Z-address interval of the query window.

A. Augment with the piecewise function

GLIN equips a piecewise function as an add-on to support the *Intersects* relationship. This function consists of a number of pieces each of which represents a subdomain of the $Zmax$ addresses of indexed geometries (i.e., $Zmax_{GM}$). When given a lookup key, the function finds the minimum $Zmin$ address of geometries (i.e., minimum $Zmin_{GM}$) in the corresponding subdomain. Below is an example piecewise function built upon the intervals from Figure 1:

$$f(Zmax_{GM}) = \begin{cases} 1 & 2 \leq Zmax_{GM} \leq 5 \\ 3 & 5 < Zmax_{GM} \leq 9 \\ 0 & 9 < Zmax_{GM} \leq 12 \\ 12 & 12 < Zmax_{GM} \leq 14 \end{cases}$$

GLIN augments the query window (Q) to incorporate the missing data (see the yellow path in Figure 1). More precisely, with the help of this piecewise function, GLIN reduces the $Zmin$ of the query window (i.e., $Zmin_Q$) such that this larger Z-address interval will cover the $Zmin$ of the geometries whose $Zmax$ satisfy either one of the following OR conditions (i.e., OR Condition 2 and 3 in Lemma 2): (1) $Zmin_Q \leq Zmax_{GM} \leq Zmax_Q$, OR (2) $Zmax_Q \leq Zmax_{GM}$. With this in mind, we can merge these two conditions to $Zmin_Q \leq Zmax_{GM}$. GLIN then uses the augmented query window to perform the index search described in Section VI. As a result, the index probing may return more false positives to be pruned but does not have true-negatives for *Intersects* relationship.

As depicted in Algorithm 2, to augment a query window, GLIN will first find the piece where $Zmin_Q$ falls in, using a binary search on the piecewise function. All geometries belonging to the pieces after this piece (including this piece itself) will satisfy $Zmin_Q \leq Zmax_{GM}$. Then GLIN will obtain the minimum $Zmin_{GM}$ among these pieces (recall that $Zmin_{GM}$ in each piece is already the minimum one for this piece). Finally, $Zmin_Q$ will be updated to the minimum $Zmin_{GM}$. In practice, this augmentation does not significantly reduce $Zmin_Q$ as $Zmin_{GM}$ and $Zmax_{GM}$ are usually close to each other (see Figure 5) and the $Zmin_{GM}$ in later pieces are less likely to be smaller than the current $Zmin_Q$.

Algorithm 2: Augment the query window

Input : $Zmin_Q, Zmax_Q$, piecewise function PW
Output: Augmented $Zmin_Q, Zmax_Q$

```

1 /* Find pieces that satisfy  $Zmin_Q \leq Zmax_{GM}$  */
2 iterator =  $PW.binary\_search(Zmin_Q)$ ;
3  $minZmin_{GM}$  = positive infinity;
4 /* Find the minimum  $Zmin_{GM}$  among pieces */
5 while iterator  $\leq PW.end()$  do
6    $minZmin_{GM} = \min(iterator.Zmin, minZmin_{GM})$ ;
7   iterator++;
8 /* Update  $Zmin_Q$  */
9  $Zmin_Q = minZmin_{GM}$ ;
10 Return  $Zmin_Q, Zmax_Q$ ;

```

Input: [Zmin, Zmax] sorted by Zmax		Piecewise function			
	Domain	Zmax _{end}	Min _{Zmin}	Sum _{Zmin}	Count
[1, 2]	{ [2, 5]	2	sentinel	sentinel	sentinel
[2, 3]		5	min{1,2,4} = 1	sum{1,2,4} = 7	3
[4, 5]					
[3, 6]	{ [5, 9]	9	min{3,5,3} = 3	sum{3,5,3} = 11	3
[5, 7]					
[3, 9]		{ (9, 12]	12	min{8,0,9} = 0	sum{8,0,9} = 17
[8, 10]					
[0, 12]	{ [12, 14]		14	min{12} = 12	sum{12} = 12
[9, 12]					
[12, 14]					

Fig. 4: Init. a piecewise function. Piece_limitation = 3.

B. Initialize the piecewise function

To create the piecewise function, GLIN sorts the geometries by their $Zmax$ addresses as each piece represents a subdomain of $Zmax$. The sorting result created for building the hierarchical model cannot be reused here because it is based on $Zmin$ addresses. To save space, GLIN will drop the $Zmax$ based sorting result once it creates the piecewise function.

As shown in Figure 4, after sorting the geometries, GLIN will start to traverse the results and creates a piece for every k geometries. In this paper, we call k as *piece_limitation* which is a tunable parameter in GLIN. This parameter sets the number of records that are summarized in a single piece when initializing the piecewise function. A higher *piece_limitation* will result in less pieces in a piecewise function, but the augmented query window will be larger and introduce more false positives for the refinement phase.

GLIN stores these pieces in a vector and each piece contains the following four aggregates: (1) $Zmax_{end}$: this indicates the upper bound of the piece's $Zmax$ domain. This value (inclusive), together with the $Zmax_{end}$ (exclusive) in the previous piece, composes the domain of this piece. (2) Min_{Zmin} : this is the minimum $Zmin$ of all geometries in this piece. (3) Sum_{Zmin} : this sums up all $Zmin$ values in this piece. (4) Count: this indicates the total number of records summarized by this piece. In fact, GLIN only needs the $Zmax_{end}$ and Min_{Zmin} values for augmenting queries. The other two values stored in this vector will be in use when GLIN maintains the piecewise function for data updates.

It is also worth noting that GLIN or learned indexes in general are data-aware and hence are not immune to complex data

distribution and data outliers (e.g., an abnormal large geometry that yields large Z_{itvl}). However, our experiments later prove that it adapts to many realistic data and Figure 5 also shows that the CDFs of Z_{min} and Z_{max} are almost identical on real-world datasets. Moreover, the piecewise function can hardly be affected by an outlier because: (1) An outlier only affects the Z_{min} of the piece when its Z_{max} is ranked the first few records in the piece. Otherwise, its Z_{min} will be absorbed by others. (2) Even if the Z_{min} of a piece is significantly changed, its value is still likely larger than the Z_{mins} of the pieces ahead of it. Thus, the impact of this outlier is again mitigated.

C. Maintain the piecewise function

When the underlying data receives updates, in addition to updates of the index structure, GLIN also needs to bring the piecewise function up-to-date to guarantee the query accuracy.

In-bound insertion. An insertion will be considered as in-bound if the Z_{max} address of the newly inserted geometry is within the current domain of the entire dataset (e.g., domain [2, 14] from Figure 4). GLIN will first locate the affected piece by performing a binary search on the piecewise function, and then update the following aggregates in this piece to incorporate the new geometry: (1) $\text{Min}_{Z_{min}} = \min \{\text{Min}_{Z_{min}}, \text{new } Z_{min}\}$; (2) $\text{Sum}_{Z_{min}} = \text{Sum}_{Z_{min}} + \text{new } Z_{min}$; (3) $\text{Count} = \text{Count} + 1$. GLIN does not create new pieces for in-bound insertion as we cannot determine the subdomain for the new piece.

Out-of-bound insertion. An insertion will be considered as out-of-bound if it is not qualified for in-bound insertion. An out-of-bound insertion only affects either the first piece or the last piece. There are two possible scenarios: (1) Count in the affected piece $\neq \text{piece_limitation}$: GLIN will treat it in the same way as in-bound insertion and hence update $\text{Min}_{Z_{min}}$, $\text{Sum}_{Z_{min}}$, and Count accordingly. (2) Count in the affected piece $= \text{piece_limitation}$: GLIN will create a new piece record at the beginning (if out of lower bound) or the end (if out of upper bound) of the current piecewise function to incorporate the new geometry.

Deletion. GLIN will first find the affected piece by performing a binary search on the piecewise function with the Z_{max} address of the deleted geometry. It will then update the following aggregates in this piece to reflect this deletion: (1) $\text{Sum}_{Z_{min}} = \text{Sum}_{Z_{min}} - Z_{min}$ of the deleted geometry. (2) $\text{Count} = \text{Count} - 1$. A piece record can be deleted when Count becomes 0. $\text{Min}_{Z_{min}}$ will not be updated as Min is considered a non-invertible aggregate [28].

Re-build the piecewise function. Although the piecewise function can always guarantee the query accuracy when data updates happen, GLIN might show performance downgrade in index search if it receives too many in-bound insertion. The reason is that in-bound insertion may make a piece summarize more geometries than what piece_limitation would allow, so the augmented query window will introduce more false positives. To remedy that, GLIN offers its user the average

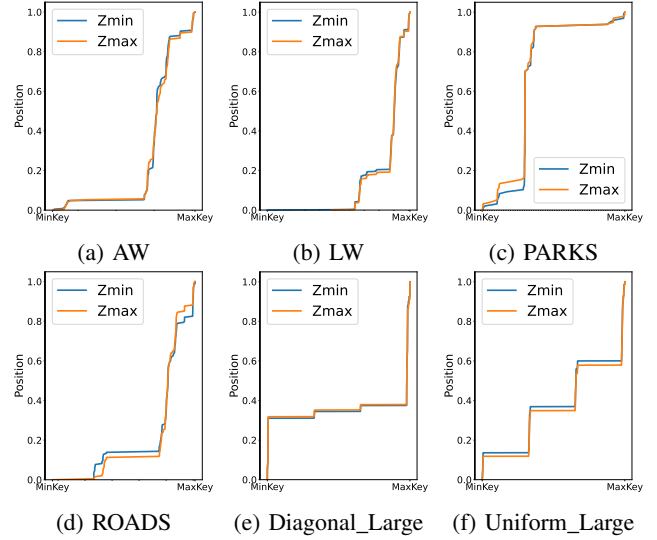


Fig. 5: CDFs of different datasets based on Z_{min} and Z_{max}

TABLE IV: Dataset description

Name	Size	Cardinality	Type	Description
AREAWATER (AW) [29]	2.27GB	2.3M	Polygon	Boundaries of water areas such as lakes in the USA
LINEARWATER (LW) [29]	6.44GB	5.8M	LineString	Paths of rivers in the USA
Roads [29]	8.29GB	19M	LineString	Paths of roads in the USA
OSM_Points (OSM) [30]	2.63GB	10M	Points	All points on the planet, 1% sample from the original data
Parks [30]	8.53GB	9.8M	Polygon	Boundaries of parks and green areas on the planet
Diagonal_Small (DIAG_S) [31]	2.04GB	10M	Polygon	A synthetic dataset following the diagonal distribution
Diagonal_Large (DIAG_L) [31]	8.14GB	40M	Polygon	A synthetic dataset following the diagonal distribution
Uniform_Small (UNIF_S) [31]	2.04GB	10M	Polygon	A synthetic dataset following the uniform distribution
Uniform_Large (UNIF_L) [31]	8.14GB	40M	Polygon	A synthetic dataset following the uniform distribution

difference function of the piecewise function:

$$\text{avg_diff} = \frac{\sum_{i=1}^n \frac{|i's \text{Min}_{Z_{min}} - i's \text{Avg}_{Z_{min}}|}{i's \text{Avg}_{Z_{min}}}}{n}$$

where $\text{Avg}_{Z_{min}} = \frac{\text{Sum}_{Z_{min}}}{\text{Count}}$, n is the total number of pieces in the piecewise function and i represents a single piece. avg_diff indicates the average difference between $\text{Min}_{Z_{min}}$ and $\text{Avg}_{Z_{min}}$ among all pieces. The user can periodically invoke this helper function to check the status. If avg_diff becomes much higher at some point, the user can ask GLIN to re-build the piecewise function.

IX. EXPERIMENTS

This section presents the result of an experimental analysis on GLIN. All experiments are done in the main memory of an iMac 2019 (Big Sur 64-bit) machine with an Intel core i3 3.6GHz Quad-Core CPU, and 32 GB DDR4 memory.

A. Experiment setup

Implementation details. To demonstrate the performance, we implement GLIN on top of ALEX using C++ since ALEX is open-source and supports data updates. Our implementation re-uses the hierarchical model and gapped arrays from ALEX and keeps the corresponding ALEX parameters unchanged.

TABLE V: Piecewise function size for non-point datasets on different Piece_Limitation (PL). Default PL = 10000

Dataset	PL=100	PL=1000	PL=10000	PL=100000
AW	716.5KB	71.65KB	7.15KB	0.72KB
LW	1824.5KB	182.5KB	18.25KB	1.85KB
ROADS	6122.7KB	612.3KB	61.22KB	6.13KB
PARKS	3072.3KB	307.25KB	30.72KB	3.06KB
DIAG_S, UNIF_S	3125KB	312.5KB	31.25KB	3.13KB
DIAG_L, UNIF_L	12500KB	1250KB	125KB	12.5KB

With that being said, GLIN can be easily migrated to other learned indexes too.

Compared approaches. (1) Boost-Rtree: from Boost C++ [32] version 1.73.0, with default settings. (2) Quad-Tree: from GEOS [33] version 3.9.0. Quad-Tree shows abnormal performance on OSM point dataset and synthetic datasets: its index size is 10X and 100X smaller than GLIN and R-Tree, and its index search time is more than 10 times longer than other approaches on 0.01% and 0.001% selectivities. Thus we exclude the results of Quad-Tree on these datasets for a fair comparison. This issue will be reported to the GEOS community. (3) GLIN: the proposed approach in this paper, without the piecewise function. This will be used for all queries with the *Contains* relationship. (4) GLIN-piecewise: the proposed approach in this paper with the piecewise function for query augmentation. This will be used for queries with the *Intersects* relationship.

Datasets. We test our approaches on 5 real-world datasets and 4 synthetic datasets (see Table IV), including point, polygon and line string data. Real-world datasets are obtained from the US Census Bureau TIGER project [29] and OpenStreetMap [30]. These datasets are cleaned by SpatialHadoop [34] and posted on their website. We generate the synthetic datasets using SpiderWeb [31] with different distributions. For point data, we only test GLIN on the *Contains* relationship as *Intersects* relationship does not apply to points.

Query selectivity. We test GLIN on 4 range query selectivities: 1%, 0.1%, 0.01%, 0.001%. To generate a range query with the required selectivity, we randomly take a geometry from the dataset and do a K Nearest Neighbor query around this geometry ($K = \text{selectivity} * \text{dataset cardinality}$) using JTS STR-Tree [35]. The MBR of the KNN query results then becomes the query window at this selectivity. We generate 100 such query windows per selectivity per dataset.

Query response time. The measured query response time consists of two parts: (1) index probing time. For all compared approaches, this is the time spent on searching the index structure. For GLIN-piecewise, this also includes the query augmentation time. (2) Refinement time. For all compared approaches, this is the time spent on refining the query results using the exact shapes of query windows and geometries. For the *Contains* relationship, the results are refined using the *Contains* check in GEOS while for the *Intersects* relationship, the refinement uses the *Intersects* check.

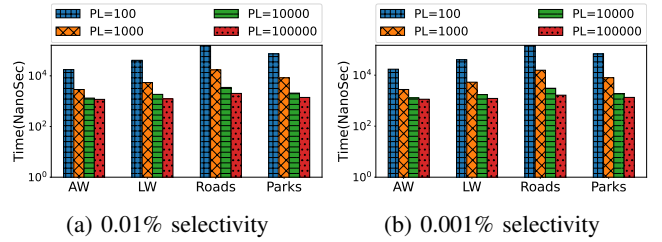


Fig. 6: GLIN index probing time on different PL (log scale)

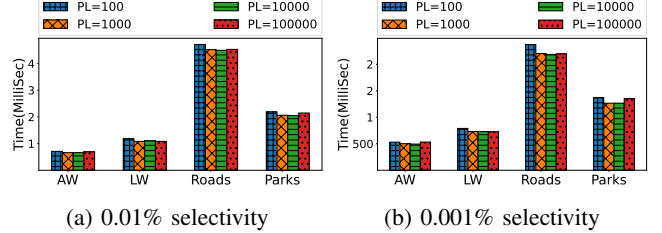


Fig. 7: GLIN query response time on diff. PL (*Intersects*)

B. Tuning GLIN parameters

This section studies the impact of the piece_limitation (PL) parameter. This parameter defines the number of records summarized by each piece of the piecewise function.

Index probing time. As shown in Figure 6, piece_limitation has a significant impact on the index probing time. Such time on piece_limitation = 100 is up to 10 times higher than that on piece_limitation = 100000. A lower piece_limitation causes a higher index probing time because the resulting piecewise function will have more pieces and hence increase the time spent on searching the piecewise function.

Index size. As depicted in Table V, the growth rate of the piecewise function size is proportional to that of the piece_limitation, which makes sense. Compared to the index size of GLIN (see Figure 8), the storage overhead of the piecewise function is negligible when piece_limitation ≥ 10000 .

Query response time. Figure 7 shows that the query response time will increase if the piece_limitation is too high or too low. This makes sense because although a higher piece_limitation value speeds up the piecewise function search in the index probing, it enlarges the augmented query window and introduces more false positives to be filtered in the refinement phase.

Therefore, in the remaining experiments, we use piece_limitation = 10000 as the default parameter as it shows the good performance in Figure 7 and its piecewise function size is very small compared to GLIN index size.

C. Indexing overhead

Index size. We measure the sizes by adding internal node size and leaf node metadata size together. As demonstrated in Figure 8, the index size of GLIN is 40 - 70 times smaller than Quad-Tree and 10 - 30 times smaller than R-Tree on real-world datasets. This makes sense because GLIN has much less nodes and each internal node uses a simple linear regression

TABLE VI: Number of nodes in compared approaches

	Boost R-TREE	Quad-Tree	GLIN
AW	244686	4777004	43701
LW	626472	5036441	57563
ROADS	2135698	14584732	103750
PARKS	626472	7366032	85922

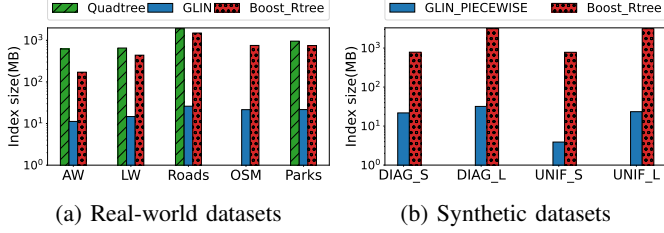


Fig. 8: Index size w/o the piecewise function (log. scale)

model which only consists of two parameters (see Figure VI). In addition, the size of GLIN piecewise function (see Table V) is very small so it does not change our conclusion.

Index initialization time. As depicted in Figure 9, GLIN consumes 10% - 50% more initialization time as opposed to Quad-Tree and R-Tree on real-world datasets. This makes sense because when initializing the index, GLIN needs to sort geometries by their Z_{min} values and train models. GLIN-piecewise takes around 10% more time than GLIN because it needs to sort geometries one more time by their Z_{max} values for generating the piecewise function.

D. Query response time

Index probing time. As shown in Figure 10, on 1% - 0.1% selectivity, the index probing time of GLIN and GLIN-piecewise is 10 - 100 times shorter than Quad-Tree. On 0.001% selectivity, GLIN and GLIN-piecewise are still 5 times and 10 times faster than R-Tree and Quad-Tree. This makes sense because GLIN uses the model prediction-based traversal while Quad-Tree and R-Tree do the comparison-based tree traversal. The index probing time of GLIN-piecewise is higher than GLIN since it needs more time to search the piecewise function and augment the query window.

Query response time. GLIN no longer has orders of magnitude difference than other indexes in terms of query response time, because the refinement phase usually takes much more time than the index probing phase when querying

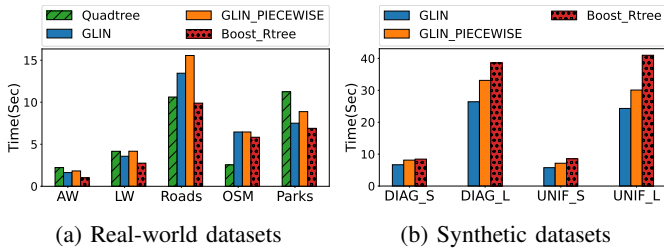


Fig. 9: Index initialization time

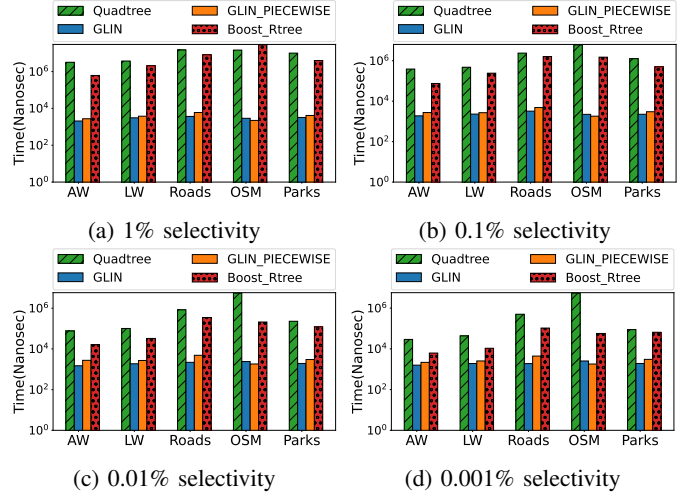


Fig. 10: Index probing time, diff. query selectivity (log. scale)

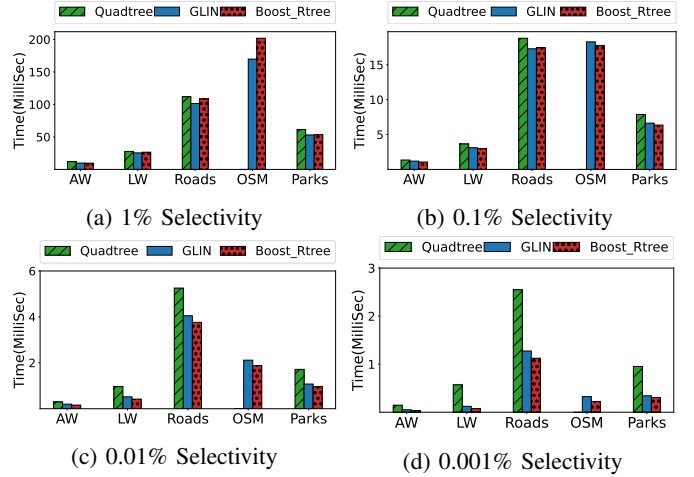


Fig. 11: Query response time on different query selectivities with *Contains* relationship

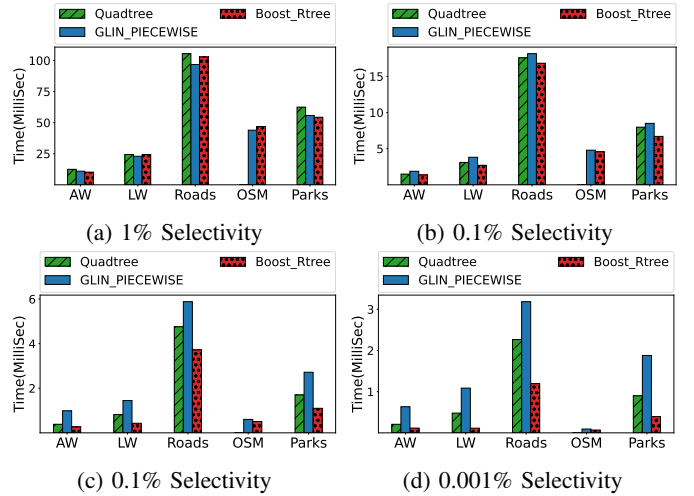


Fig. 12: Query response time on different query selectivities with *Intersects* relationship

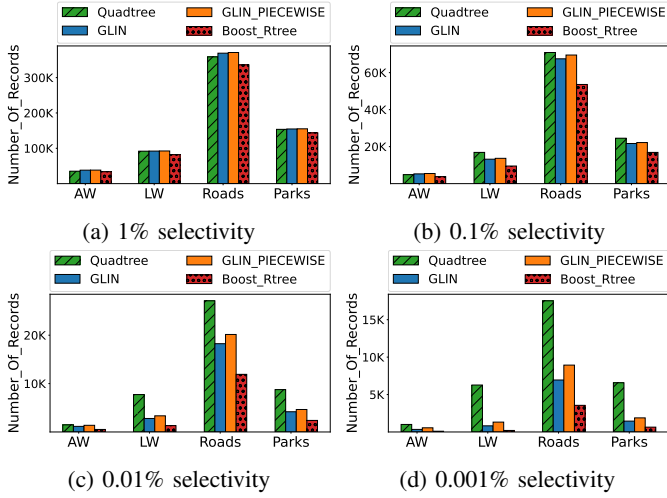


Fig. 13: Number of records checked during the refinement

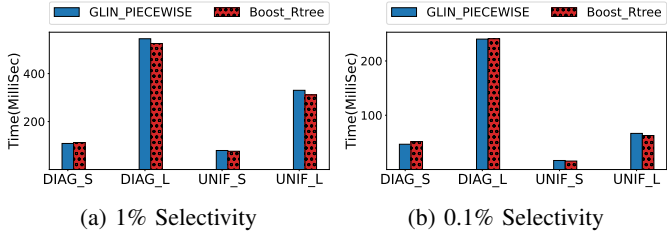


Fig. 14: Query response time on synthetic data (*Intersects*)

complex geometries [23]. Figure 11 shows that, for *Contains* relationship, GLIN has a similar or shorter query response time compared to Quad-Tree on almost all selectivities because it has less false positives to refine. GLIN has similar query response time compared to R-Tree on 1% to 0.1% selectivity but is 10% slower on 0.01% and 0.001% selectivity because R-Tree has less false positives. Figure 12 and 14 show that, for *Intersects* relationship, GLIN-piecewise has similar query response compared to Quad-Tree and R-Tree on 1% to 0.1% selectivity. On 0.01% and 0.001% selectivity, GLIN-piecewise are 10% - 20% slower than Quad-Tree and 1 to 2 times slower than R-Tree. This is because the augmented query window in GLIN-piecewise introduces more false positives and hence slows down the refinement.

False positives. Figure 13 illustrates the number of records checked during the refinement. A lower value indicates less false positives which eventually leads to less refinement time and overall query response time. GLIN has 10% - 20% more false positives than R-Tree on 1% and 0.1% selectivity. But the fast index probing of GLIN makes up the difference so its query response time is similar to others. As expected, GLIN-piecewise introduces more false positives. Another observation is that although on 0.01% and 0.001% selectivity, GLIN has less records to check but still costs more than Quad-Tree. This is because checking leaf MBRs in GLIN also costs time.

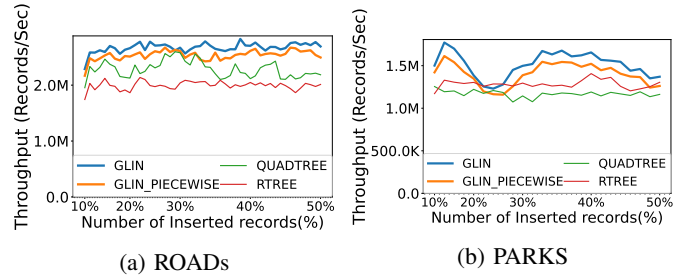


Fig. 15: Index insertion performance on different datasets

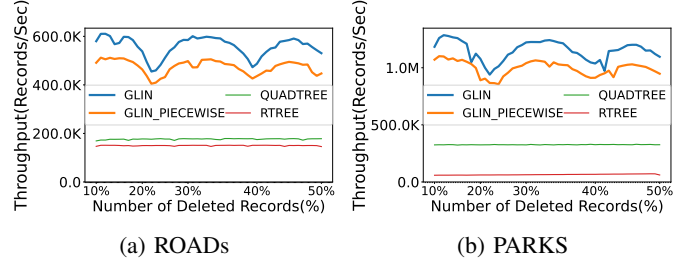


Fig. 16: Index deletion performance on different datasets

E. Maintenance Overhead

Insertion. For each dataset, we first bulk-load a random 50% of the data into all indexes and then insert the remaining 50% into the indexes record by record. As shown in Figure 15, on larger datasets, the throughput of GLIN is around 1.5 times higher than R-Tree and 1.2 times higher than Quad-Tree. This makes sense because GLIN's index probing is orders of magnitude faster than others (see Figure 11) and no refinement is needed for insertion. GLIN-piecewise is around 10% slower than GLIN because it needs to update the piecewise function as well. GLIN occasionally show performance downgrade because of node expansion or splitting.

Deletion. For each dataset, we first bulk-load the entire dataset and then randomly delete 50% of the data record by record. As shown in Figure 16, on larger datasets, the throughput of GLIN is around 3 - 5 times higher than R-Tree and Quad-Tree because GLIN's index probing is orders of magnitude faster than other indexes. The throughput of GLIN-piecewise is around 20% lower than GLIN as it has to update the piecewise function. GLIN occasionally show performance downgrade because of node merging.

F. Hybrid workload

We define a transaction as (1) query: a spatial range query with *Intersects* relationship at 1% selectivity, or (2) insertion: insert 1% new records into the indexes. We have two hybrid workloads: (1) read-intensive: 90% of the transactions are queries and the other 10% are insertion. (2) Write-intensive: 50% of the transactions are queries and the rest are insertion. For each dataset, we first bulk-load 50% of the entire dataset, and then start the workloads. We stop when the remaining 50% data are inserted.

Read-intensive workload. As shown in Figure 17a and 17b, the throughput of GLIN-piecewise is similar to Quad-

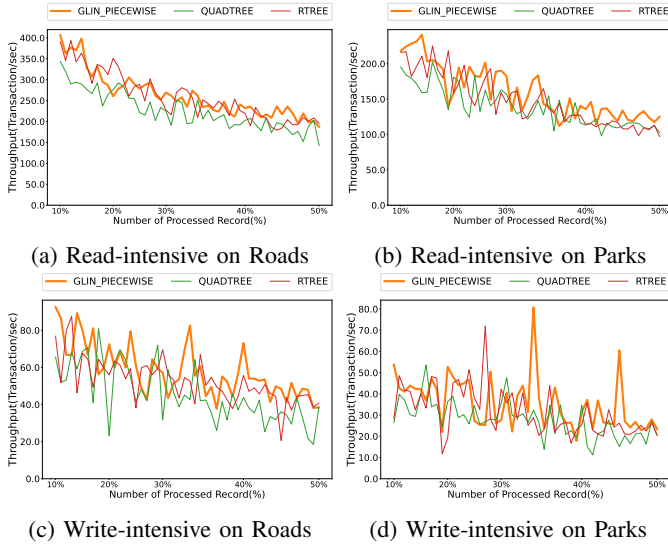


Fig. 17: Index performance on hybrid workloads

Tree and R-Tree on the read-intensive workload. This makes sense because GLIN-piecewise has similar query performance as other indexes (see Figure 12a) and the throughput mainly reflects the query performance on the read-intensive workload.

Write-intensive workload. As shown in Figure 17c and 17d, GLIN-piecewise outperforms Quad-Tree and R-Tree almost all the time. This matches our expectation because the insertion speed of GLIN-piecewise is much higher than that of Quad-Tree and R-Tree (see Figure 15). When we have a write-intensive workload, the overall performance of GLIN-piecewise is proven to be better.

X. RELATED WORK

Learned indexes. Researchers from Google and MIT [14] propose to use machine learning models to replace the complex tree index as B+Tree. They design a recursive model index(RMI), a tree-like hierarchical model, to learn the cumulative distribution function(CDF) between keys and their position. RMI takes as input a lookup key and predicts the corresponding position by using the models level by level. Compared to B+ Tree, RMI possesses low storage overhead with an outperforming lookup performance but only supports read-only workload. Hermit [15] is a learned secondary index that leverages a hierarchical machine learning model to learn the correlation between two columns. ALEX [16] is an updatable learned index which adopts RMI's hierarchy structure but adds gapped arrays and node splitting to absorb data updates.

Learned spatial indexes. Researchers have been working on extending learned indexes to uphold spatial and multi-dimensional point data. SageDB [36] introduces a learned database system with a learned multidimensional index embedded. This work sorts and partitions data points according to each dimension. ZM-index [19] leverages the Z-order space-filling curve to sort the data and then builds RMI on them. Given a spatial range query, it first maps a range query to

two Z addresses, then uses the prebuilt machine learning model to find an approximate range for further investigation. Although both GLIN and ZM-Index make use of Z order curve, ZM-index cannot handle non-point data and only works with read-only workload. Flood [17] also employs the RMI to support multidimensional data. It proposes an in-memory read optimized index that partitions a d-dimensional space with a d-1 dimensional grid. The model will predict the grid cell that contains the lookup key. The ML-Index [37] utilizes the iDistance [38] to map data points to the one-dimensional value and also employs the RMI to index the values further. Qi et al. [39] come up with a recursive spatial model index called RSMI to improve the ZM-index. Their work mitigates the uneven gap problem by using a rank space-based transformation. However, this work provides approximate answers. Li et al. propose LISA [18], a disk-based learned spatial index that can reach a low storage consumption and I/O cost. LISA partitions the space to grids and assigned each grid an ID by applying the partially monotonic function. All of the works mentioned above focus on making learned indexes work for 2 or multi-dimensional point data. Unfortunately, in the real world, geospatial data is more than just points. GLIN handles all types of geometries and hence is a practical alternative to R-Tree or Quad-Tree.

Lightweight index structures. Researchers [40], [41] have been making use of classic compression techniques to drop repeated information stored in B+ Tree and R-Tree tree nodes. Although compressed indexes shrink the index size, they do not reduce the complexity of the index structure and even increase the query response time and maintenance time due to additional compression and decompression steps. Some other studies focus on succinct index structures which take advantage of data synopses from the indexed data and quickly skip irrelevant data. Column imprints [11] utilizes the idea of cache conscious bitmap indexing to create a bit map for each zone. Block Range Indexes (BRIN) [42] stores min/max values for each range of disk blocks. Hippo [13] extends BRIN's idea but implements partial histograms in each range to decrease the query response time. Hentschel et al. propose Column Sketch [12] that makes use of lossy compression to generate data synopses and hence accelerates table scan. BF-tree [43] applies bloom filter in the leaf node of a B-Tree and hence reduces the storage overhead. However, these succinct index structures reduce the index storage overhead at the cost of additional query response time and cannot be easily tailored to complex geometries.

XI. CONCLUSION

This paper introduces GLIN, a lightweight learned index for spatial range queries on complex geometries. In terms of storage overhead, GLIN is 40 - 70 times less than Quad-Tree and 10 - 30 times less than R-Tree. Moreover, GLIN's maintenance speed is around 1.5 times higher on insertion and 3 - 5 times higher on deletion as opposed to R-Tree and Quad-Tree. If the application only needs the *Contains* relationship, the user can opt to use GLIN without query augmentation

because it shows similar query response time than Quad-Tree and R-Tree in most cases. GLIN with query augmentation deals with both spatial relationships while showing competitive performance on 1% and 0.1% query selectivity. In a nutshell, GLIN is a lightweight indexing mechanism for medium selectivity queries which are commonly used in spatial analytics applications. In the future, we will plan to extend GLIN to support K Nearest Neighbor queries.

REFERENCES

- [1] A. Guttman, “R-trees: A dynamic index structure for spatial searching,” in *Proceedings of the ACM International Conference on Management of Data, SIGMOD*. ACM Press, 1984, pp. 47–57.
- [2] J. L. Bentley, “Multidimensional binary search trees used for associative searching,” *The Communications of the ACM*, vol. 18, no. 9, pp. 509–517, 1975.
- [3] H. Samet, “The quadtree and related hierarchical data structures,” *ACM Computing Surveys, CSUR*, vol. 16, no. 2, pp. 187–260, 1984.
- [4] J. Yu and M. Sarwat, “Indexing the pickup and drop-off locations of NYC taxi trips in postgresql - lessons from the road,” in *Proceedings of the International Symposium on Advances in Spatial and Temporal Databases, SSTD*, ser. Lecture Notes in Computer Science, vol. 10411. Springer, 2017, pp. 145–162.
- [5] M. Olma, F. Tauheed, T. Heinis, and A. Ailamaki, “BLOCK: efficient execution of spatial range queries in main-memory,” in *Proceedings of the International Conference on Scientific and Statistical Database Management, SSDBM*. ACM, 2017, pp. 15:1–15:12.
- [6] D. Tsitsigkos, K. Lampropoulos, P. Boursos, N. Mamoulis, and M. Terrovitis, “A two-layer partitioning for non-point spatial data,” in *Proceedings of the International Conference on Data Engineering, ICDE*. IEEE, 2021, pp. 1787–1798.
- [7] “Apache parquet,” <https://parquet.apache.org/>.
- [8] “Geoparquet,” <https://github.com/opengeospatial/geoparquet>.
- [9] “Delta lake,” <https://delta.io/>.
- [10] “Apache iceberg,” <https://iceberg.apache.org/>.
- [11] L. Sidirourgos and M. L. Kersten, “Column imprints: a secondary index structure,” in *Proceedings of the ACM International Conference on Management of Data, SIGMOD*. ACM, 2013, pp. 893–904.
- [12] B. Hentschel, M. S. Kester, and S. Idreos, “Column sketches: A scan accelerator for rapid and robust predicate evaluation,” in *Proceedings of the ACM International Conference on Management of Data, SIGMOD*. ACM, 2018, pp. 857–872.
- [13] J. Yu and M. Sarwat, “Two birds, one stone: A fast, yet lightweight, indexing scheme for modern database systems,” *Proceedings of the VLDB Endowment, PVLDB*, vol. 10, no. 4, pp. 385–396, 2016.
- [14] T. Kraska, A. Beutel, E. H. Chi, J. Dean, and N. Polyzotis, “The case for learned index structures,” in *Proceedings of the ACM International Conference on Management of Data, SIGMOD*. ACM, 2018, pp. 489–504.
- [15] Y. Wu, J. Yu, Y. Tian, R. Sidle, and R. Barber, “Designing succinct secondary indexing mechanism by exploiting column correlations,” in *Proceedings of the ACM International Conference on Management of Data, SIGMOD*. ACM, 2019, pp. 1223–1240.
- [16] J. Ding, U. F. Minhas, J. Yu, C. Wang, J. Do, Y. Li, H. Zhang, B. Chandramouli, J. Gehrke, D. Kossmann, D. B. Lomet, and T. Kraska, “ALEX: an updatable adaptive learned index,” in *Proceedings of the ACM International Conference on Management of Data, SIGMOD*. ACM, 2020, pp. 969–984.
- [17] V. Nathan, J. Ding, M. Alizadeh, and T. Kraska, “Learning multi-dimensional indexes,” in *Proceedings of the ACM International Conference on Management of Data, SIGMOD*. ACM, 2020, pp. 985–1000.
- [18] P. Li, H. Lu, Q. Zheng, L. Yang, and G. Pan, “LISA: A learned index structure for spatial data,” in *Proceedings of the ACM International Conference on Management of Data, SIGMOD*. ACM, 2020, pp. 2119–2133.
- [19] H. Wang, X. Fu, J. Xu, and H. Lu, “Learned index for spatial queries,” in *Proceedings of the International Conference on Mobile Data Management, MDM*. IEEE, 2019, pp. 569–574.
- [20] V. Pandey, A. van Renen, A. Kipf, J. Ding, I. Sabek, and A. Kemper, “The case for learned spatial indexes,” in *AIDB@VLDB 2020, 2nd International Workshop on Applied AI for Database Systems and Applications, Held with VLDB 2020, Monday, August 31, 2020, Online Event / Tokyo, Japan*, 2020.
- [21] J. Yu, Z. Zhang, and M. Sarwat, “Spatial data management in apache spark: the geospark perspective and beyond,” *GeoInformatica*, vol. 23, no. 1, pp. 37–78, 2019.
- [22] “ISO/IEC 13249-3:2016 Information technology — Database languages — SQL multimedia and application packages — Part 3: Spatial,” <https://www.iso.org/standard/60343.html>.
- [23] P. Boursos and N. Mamoulis, “Spatial joins: what’s next?” *ACM SIGSPATIAL Special*, vol. 11, no. 1, pp. 13–21, 2019.
- [24] A. Kipf, R. Marcus, A. van Renen, M. Stoian, A. Kemper, T. Kraska, and T. Neumann, “Radixspline: a single-pass learned index,” in *Proceedings of the ACM International Conference on Management of Data, SIGMOD*. ACM, 2020, pp. 5:1–5:5.
- [25] “Libmorton library,” <https://github.com/Forceflow/libmorton>.
- [26] K. C. K. Lee, B. Zheng, H. Li, and W. Lee, “Approaching the skyline in Z order,” in *Proceedings of the International Conference on Very Large Data Bases, VLDB*. ACM, 2007, pp. 279–290.
- [27] “Accuracy versus decimal places,” http://wiki.gis.com/wiki/index.php/Decimal_degrees.
- [28] J. Traub, P. M. Grulich, A. R. Cuellar, S. Breß, A. Katsifodimos, T. Rabl, and V. Markl, “Efficient window aggregation with general stream slicing,” in *Proceedings of the International Conference on Extending Database Technology, EDBT*. OpenProceedings.org, 2019, pp. 97–108.
- [29] “TIGER/Line files,” <http://www.census.gov/geo/www/tiger/>.
- [30] “OpenStreetMap,” <http://www.openstreetmap.org/>.
- [31] P. Katiyar, T. Vu, and A. Eldawy, “Spiderweb: A spatial data generator on the web,” in *International Conference on Advances in Geographic Information Systems*. ACM, 2020, pp. 465–468.
- [32] R. R. Beman Dawes, David Abrahams. boost c++ library. [Online]. Available: <https://www.boost.org/>
- [33] GEOS contributors, *GEOS coordinate transformation software library*, Open Source Geospatial Foundation, 2021. [Online]. Available: <https://libgeos.org/>
- [34] A. Eldawy and M. F. Mokbel, “SpatialHadoop: A MapReduce Framework for Spatial Data,” in *Proceedings of the International Conference on Data Engineering, ICDE*, 2015, pp. 1352–1363.
- [35] M. Davis. Jts topology suite. [Online]. Available: <http://locationtech.github.io/jts/>
- [36] T. Kraska, M. Alizadeh, and A. Beutel, “Sagedb: A learned database system,” in *Proceedings of the International Conference on Innovative Data Systems Research, CIDR*. www.cidrdb.org, 2019.
- [37] A. Davitkova, E. Milchevski, and S. Michel, “The ml-index: A multidimensional, learned index for point, range, and nearest-neighbor queries,” in *Proceedings of the International Conference on Extending Database Technology, EDBT*. OpenProceedings.org, 2020, pp. 407–410.
- [38] H. V. Jagadish, B. C. Ooi, and K. Tan, “idistance: An adaptive b⁺-tree based indexing method for nearest neighbor search,” *ACM Trans. Database Syst.*, vol. 30, no. 2, pp. 364–397, 2005.
- [39] J. Qi, G. Liu, C. S. Jensen, and L. Kulik, “Effectively learning spatial indices,” *Proceedings of the VLDB Endowment, PVLDB*, vol. 13, no. 11, pp. 2341–2354, 2020.
- [40] G. Graefe and H. A. Kuno, “Modern b-tree techniques,” in *Proceedings of the International Conference on Data Engineering, ICDE*. IEEE Computer Society, 2011, pp. 1370–1373.
- [41] J. Goldstein, R. Ramakrishnan, and U. Shaft, “Compressing relations and indexes,” in *Proceedings of the International Conference on Data Engineering, ICDE*. IEEE Computer Society, 1998, pp. 370–379.
- [42] M. Stonebraker and L. A. Rowe, “The design of postgres,” in *Proceedings of the ACM International Conference on Management of Data, SIGMOD*. ACM Press, 1986, pp. 340–355.
- [43] M. Athanassoulis and A. Ailamaki, “Bf-tree: Approximate tree indexing,” *Proceedings of the VLDB Endowment, PVLDB*, vol. 7, no. 14, pp. 1881–1892, 2014.